Invited Paper

Laser-array generators produced by patterned ion irradiation of acrylic films

Brian G. Hoover[a], Chase K. McMichael[b], Lowell T. Wood[c], Zuhua Zhang[b,c], Jia-Rui Liu[b,c], and Wei-Kan Chu[b,c]
[a]Advanced Optical Technologies, Albuquerque, NM USA
[b]Texas Center for Superconductivity at the University of Houston, Houston, TX USA
[c]Department of Physics, University of Houston, Houston, TX USA

ABSTRACT

Ion irradiation of polymer films is a promising process technology for photonics applications that require flexible, lightweight devices resistant to selected environmental variables. Crossed phase gratings that may serve as laser-beam array generators are fabricated using the dry process of irradiation of acrylic (PMMA) films with various doses of high-energy alpha particles through a stencil mask. The gratings are examined with the aid of AFM and SEM images, and Raman-Nath diffraction analysis is applied to estimate the generated refractive-index modulation as a function of the dose. SEM images of a stained grating cross-section suggest a mechanism of unsaturated bond formation and accompanying contraction of the irradiated polymer. Post-irradiation baking is shown to increase the contraction or generated surface relief by around an order of magnitude. Since the index modulation and surface relief due to irradiation tend to cancel, the overall diffraction efficiencies of unbaked gratings do not surpass 67%, although baked gratings can provide higher diffraction efficiencies.

Keywords: Ion irradiation, phase grating, PMMA, AFM, Raman-Nath equations

1. INTRODUCTION

Certain application areas of photonics demand robust, high-performance materials and process technologies. Applications that require lightweight, durable, and/or flexible photonic devices increasingly find solutions based on polymers, which may serve as the host medium, the device, or both. The processed polymer of a photonic device often needs to be resistant to environmental extremes in temperature, humidity, solar exposure, etc.

The demands of certain applications on the mechanical and/or chemical properties of photonic devices elicit the consideration and research of unconventional polymer materials and process technologies. A process technology applicable to a wide range of optical polymers allows device designers to select a material based on its mechanical and/or chemical properties rather than its optical properties. Two related candidate unconventional process technologies for polymer photonics are ion implantation and ion irradiation, which are distinguished by whether or not, respectively, the projectile ions come to rest within the device material. This paper describes processing by ion irradiation.

In comparison with other process technologies ion irradiation has several advantages as a fabrication tool for polymer photonics.[1,2] Ions of sufficient energy will modify the optical properties of nearly any polymer material, without the need for the dyes or activators usually required of media suitable for optical processing techniques like holography. Holographic media, for instance dichromated gelatin (DCG), are also often susceptible to environmental variables such as humidity, while polymer media suitable for processing by ion irradiation can be specified for flat behavior with selected environmental variables. Additionally, many ion-irradiation processes that produce useful changes in optical polymers are dry processes that require minimal use of the solvents or etchants required, for instance, in electron-beam and many optical fabrication technologies.

This paper presents a technique based on ion irradiation for the fabrication of diffractive microstructures in polymer material, more specifically two-dimensional or crossed phase gratings in acrylic films. The particular

Further author information: (Send correspondence to B. G. Hoover) E-mail: hoover@advanced-optical.com, Telephone: 1 505 250 9586 Address: PO Box 8383, Albuquerque, NM 87198 USA

Photonics for Space Environments X, edited by Edward W. Taylor, Proceedings of SPIE Vol. 5897
(SPIE, Bellingham, WA, 2005) · 0277-786X/05/$15 · doi: 10.1117/12.619144

gratings are fabricated in (poly)methylmethacrylate (PMMA) films by patterned irradiation with alpha (He^{2+}) particles at energies of 1 or 2 million electron-volts (MeV). Patterning is accomplished through the parallel process of irradiation through a stationary stencil mask, in contrast with serial processes based on a focused ion beam (FIB).[1–3] Atomic-force microscopy (AFM), scanning-electron microscopy (SEM), and measurements of laser diffraction efficiencies are applied to characterize the gratings. The thickness of the PMMA films is around $3\mu m$ to allow for diffraction analysis under the thin-grating approximation.

Crossed phase gratings may serve as laser-beam array generators. Laser-beam arrays are applicable to a wide and expanding range of tasks in the areas of optical computing and interconnection, laser communications, wavefront sensing, tracking, surveillance, and optical biometrics.

2. DEVICE DESIGN AND PRODUCTION

A diffraction grating introduces periodic modulation of an incident wave. Optical gratings usually modulate amplitude and/or phase. Phase modulation in transmission is equivalent to modulation of the optical path-length $OPL = nd$, and is therefore achieved by refractive-index modulation (Δn) and/or thickness modulation or surface relief (Δd). A binary phase grating is characterized by an OPL that assumes only the two values $n_0 d_0$ and $(n_0 + \Delta n)(d_0 + \Delta d)$ periodically. The Dammann grating is an example of a two-dimensional or crossed binary-phase grating.[4] The gratings described here are designed as crossed binary-phase gratings, although AFM measurements reveal that the generated surface relief is quasi-binary only for low irradiation doses.

Optical-grade polymers typically exhibit index modulation (Δn) and contraction (Δd) due to ion irradiation. Low-mass, high-energy ions alter the refractive index of certain optical-grade polymers without introducing appreciable absorption;[5–8] ion irradiation of polymer films is therefore applicable to the production of low-loss photonic devices such as waveguides and diffractive elements.

The devices described in this paper are designed as thin, crossed binary-phase diffraction gratings to be used in transmission. The diffraction analysis of thin transmission phase gratings is widely known as the Raman-Nath theory,[9] the applicability of which hinges on the definition of a *thin* grating as one of thickness

$$T \ll \Lambda / \tan\theta, \tag{1}$$

where Λ is the grating period and θ the internal incident angle.[10] An important assumption in the Raman-Nath theory is that the refractive-index modulation is constant throughout the thickness of the grating.

Based on knowledge of ion beam-polymer interactions irradiation parameters are chosen to produce a grating that can be approximately modeled by the Raman-Nath theory. Ion beam-solid interactions are broadly classified as either electronic or nuclear according to the mechanism of energy transfer.[11–13] For grating production the irradiation parameters are chosen to produce a nearly uniform profile of electronic energy transfer throughout the thickness of the acrylic film. The energy-transfer profiles are simulated using the TRIM code.[14] The acrylic is (poly)methylmethacrylate (PMMA) of two molecular weights MW = 34,000amu and 1,000,000amu. According to the TRIM simulations, alpha particles accelerated to 1MeV impart energy via electronic stopping to 10% uniformity throughout a 3μm PMMA film. The refractive-index modulation Δn and shrinkage Δd of PMMA due to irradiation are primarily functions of the ion fluence or dose.[15]

PMMA films were spin cast from a chlorobenzene solution onto glass slides to thicknesses of approximately 3 or 3.4μm and irradiated at normal incidence through a copper or nickel mesh composed of $5\mu m$ wires and $7.5\mu m$ spaces (2000 Mesh). The beam of alpha particles was extracted from an RF ion source and accelerated to 1-2MeV by a 5SDH-2 tandem accelerator with terminal voltage 1.7MV. The ion beam was scanned over the stencil mask and underlying film of area $\approx 150 mm^2$. The beam current density was kept $< 5\text{nA/cm}^2$ (power density $< 10\text{mW/cm}^2$) to avoid overheating without a discharge layer. The ion dose varied from $10^{12} cm^{-2}$ to $2 * 10^{14} cm^{-2}$ with an uncertainty of $\pm 3\%$ due to scanning nonuniformity. Noticeable darkening of the films occurred with doses $> 1 * 10^{14} cm^{-2}$. Following irradiation some films were baked around the glass transition temperature of PMMA $T_g = 90° - 100°C$ for 20-60 minutes. No wet chemical processing was required. An optical micrograph of a resulting patterned film is shown in Fig. 1.

3. DEVICE CHARACTERIZATION

3.1. Atomic Force Microscopy

AFM scans reveal two primary characteristics of the gratings that affect their optical performance and modeling, specifically the contraction Δd and the shape of the grating features. A determination of contraction vs. dose allows estimation of refractive-index modulation vs. dose from measurements of laser diffraction efficiencies, while the shapes of the grating features reveal something of the polymer rheological response to the irradiation as well as qualify model surfaces for diffraction analysis.

Figure 2 illustrates AFM scans over 4 grating cycles in high MW PMMA irradiated with 2MeV alpha particles to two doses. The grating profile due to low-dose irradiation is highly periodic and regular, while that due to higher doses exhibits apparently random non-periodic topographical features. The notoriously poor rheological properties of PMMA may explain the development of random topographical features at higher doses, which might therefore be suppressed under irradiation at lower beam current or lower temperature. Figure 3 provides the contraction vs. dose curve for $3.4\mu m$-thick high MW PMMA film irradiated with 2MeV alpha particles. The variation in the contraction averaged over about 30 grating cycles (error bar) increases considerably with the dose. The additional data point at $5*10^{12}cm^{-2}$ reveals that post-irradiation baking ($90°C$ for 20m) enhances the contraction of the irradiated regions by around an order of magnitude, but also introduces generally undesirable random topographical variations.

3.2. Scanning Electron Microscopy

Scanning electron microscopy (SEM) was employed to examine a low-dose post-baked grating in cross-sections perpendicular to the film plane presented in Fig. 1. SEM images of the cross-sections reveal the refractive-index modulation in the grating and provide qualitative insights into the chemical effects of the irradiation on the polymer through the atomic number (Z) contrast of stained film cross-sections.

After swatches of the grating were lifted from the glass substrate by adhesion to polyacrylic-acid (PAA) casts and embedded in epoxy, 80nm cross-sections were cut using a Reichert-Jung ultramicrotome with a glass knife. The grating sections were stained by suspension over a 50mM aqueous solution of osmium tetroxide (OsO_4) for 2 hours. OsO_4 selectively oxidizes unsaturated (C=C) bonds, the formation of which is expected in PMMA under irradiation with low-mass, high-energy ions.

Back-scattered electrons (BSE) formed the SEM images shown in Fig. 4. As oxidation of C=C bonds incorporates osmium ($Z = 76$) into the irradiated regions, these regions appear in the BSE images with high contrast relative to the unirradiated regions of pristine PMMA, which contain no unsaturated carbon bonds. The grating imaged in Fig. 4 was irradiated with $2*10^{12}/cm^2$ alpha particles at 1MeV energy and post-baked at $100°C$ for 1h. The SEM image reveals contraction of the irradiated polymer by approximately 45% in a nearly parabolic surface profile due to boundary attachment to the unirradiated material. The parabolic profile seems to develop during baking. The thickness variation from the center to the edge of the baked irradiated regions is $\approx 1\mu$m.

3.3. Optical Characterization / Diffraction Analysis

Figure 5 is a photograph of the laser spot array generated by a grating normally illuminated by a helium-neon (HeNe) laser beam of wavelength $\lambda = 632.8$nm. The parameters of the grating are $3.4\mu m$ film thickness, $1 * 10^{13}cm^{-2}$ He^{2+} 2MeV irradiation, and post-bake at $90°C$ for 20m. The overall diffraction efficiency of this grating at this wavelength is 74%. As the surface relief in baked gratings can be larger than the wavelength (see Figs. 3-4), overall diffraction efficiencies of 100% ($\eta_{00} = 0$) should be possible with appropriate post-bake parameters. AFM scans however reveal that the grating profiles in large surface relief are riddled with random topographical features, which makes diffraction analysis of these gratings difficult. The diffraction analysis is therefore limited to low-dose unbaked gratings, which present more strictly periodic profiles and precisely-measurable surface relief as indicated in the lower left portion of the plot in Fig. 3.

Optical characterization of the gratings, achieved by fitting the appropriate Raman-Nath equations to measured intensities over the laser-spot arrays, can be applied to estimate the index modulation generated in the

polymer by the ion irradiation and to infer diffraction efficiencies of gratings made with variable process parameters such as ion dose. Raman-Nath equations are derived for the ideal binary square-wave phase grating for this application.

The Raman-Nath equations are easily derived for index modulation and surface relief in overlapping square-wave profiles. Assuming illumination at normal incidence and referring to the schematic in Fig. 6, the phase modulation for transmission in this case is modeled as

$$\begin{aligned}\delta_{square}(x,y) &= (2\pi d_0/\lambda)\left[n_0 + \left\{(n_i-1)\frac{d'}{d_0} - (n_0-1)\right\} S(x,y)\right] \\ &= (2\pi d_0/\lambda)(n_0 + \Delta n' S(x,y)),\end{aligned} \tag{2}$$

where d_0 and n_0 are the thickness and refractive index of the unirradiated film, n_i is the refractive index of the irradiated film, $S(x,y)$ is the crossed square-wave modulation function, which is separable as $S(x,y) = s(x)s(y)$, and λ is the illumination wavelength. In Eq. 2 and Fig. 6 d' is an effective thickness in the irradiated regions for which the ideal square-wave grating produces a 5×5 spot array closest to that of the fabricated grating in a percentage least-squares sense over the array. The parameter d' is included to potentially account for deviations from the ideal square-wave profile, however the results presented here simply assume $d' = d_0 - \Delta d$. The effective index modulation $\Delta n'$ represents the sum of contributions of surface relief and true refractive-index modulation. With the effective modulation parameter

$$\gamma' \equiv \frac{\pi d_0 \Delta n'}{\lambda}, \tag{3}$$

the diffracted field in the far-zone of the square-wave phase grating is proportional to the Fourier transform

$$E^d_{square}(k_x,k_y) = \int\int \exp[2j\gamma' s(x)s(y)] \exp[jk_x x] \exp[jk_y y] dxdy. \tag{4}$$

With the duty-cycle $(1-a)$ and the period Λ variable but identical in the x and y directions and the unirradiated regions $a\Lambda$ on a side $(0 \le a \le 1)$, expansion of $\exp[2j\gamma' s(x)s(y)]$ as a two-dimensional Fourier series enables evaluation of the integral of Eq. 4 as

$$\begin{aligned}E^d_{square}(k_x,k_y) = &\left[1 + a^2\left(e^{2j\gamma'} - 1\right)\right]\delta(k) + 4a^2(e^{2j\gamma'} - 1) \\ &\times \sum_{l=0}^{\infty}\sum_{m=0}^{\infty} \mathrm{sinc}(la)\mathrm{sinc}(ma)\left[\delta(k_x - lK) + \delta(k_x + lK)\right]\left[\delta(k_y - mK) + \delta(k_y + mK)\right], \\ &(l+m \neq 0)\end{aligned}$$

where δ is the Dirac delta function, $\mathrm{sinc}(x) \equiv \sin(\pi x)/\pi x$, and $K \equiv 2\pi/\Lambda$. The diffraction efficiencies of the square-wave phase grating are therefore

$$\eta_{00} = 1 + 4a^2(a^2-1)\sin^2\gamma' \text{ and } \quad \eta_{lm} = \left[8a^2\,\mathrm{sinc}(la)\mathrm{sinc}(ma)\sin\gamma'\right]^2 \quad (l+m \neq 0). \tag{5}$$

As an example, the grating produced by irradiation with $1 * 10^{13} cm^{-2}$ He^{2+} of energy 2MeV diffracts the laser-spot intensities relative to the undiffracted spot

$$\eta_{meas} = \begin{bmatrix} .0001 & .0006 & .0012 & .0008 & .0002 \\ .0006 & .0036 & .0068 & .0040 & .0007 \\ .0011 & .0064 & 1 & .0065 & .0010 \\ .0008 & .0040 & .0067 & .0036 & .0006 \\ .0002 & .0008 & .0012 & .0006 & .0001 \end{bmatrix} \tag{6}$$

under normal HeNe laser illumination. Using the Raman-Nath equations 5 in a search algorithm with $a = 0.36$, $\lambda = .6328\mu m$, and $d_0 = 3.4\mu m$ provides a minimum percentage least-squared deviation from the measured spot intensities (Eq. 6) of 12.5% over the array with $\Delta n' = .0055$. The duty cycle $1-a$ is allowed to vary by 15% in

the search algorithm consistent with observed variations in the 2000 Mesh stencil mask. The spot array derived for the ideal square-wave grating with these parameters is

$$\eta_{square} = \begin{bmatrix} .0001 & .0007 & .0011 & .0007 & .0001 \\ .0007 & .0038 & .0060 & .0038 & .0007 \\ .0011 & .0060 & 1 & .0060 & .0011 \\ .0007 & .0038 & .0060 & .0038 & .0007 \\ .0001 & .0007 & .0011 & .0007 & .0001 \end{bmatrix}. \quad (7)$$

Using $n_0 = 1.490$ for the refractive index of pristine PMMA, and $\Delta d = 133nm$ from Fig. 3, the refractive index generated in PMMA at this irradiation dose is estimated as $n_i = 1.516$, or $\Delta n = .026$. Figure 7 is a plot of the refractive-index modulation Δn so derived over the lower end of the dose range examined. The 5×5 spot arrays due to ideal square-wave gratings with the parameters implied in Figs. 3 & 7 deviate in the least-squares sense from the measured spot arrays generated by the gratings irradiated with the corresponding dose as 30.6, 18.6, 17.6, 12.5, and 31.7% in ascending order.

4. DISCUSSION AND CONCLUSIONS

This paper reports on the production and basic analyses of crossed phase gratings that may serve as laser array generators, fabricated using irradiation with high-energy alpha particles through a stencil mask. The gratings and analyses are representative of an approach for the development of fabrication technologies for photonic devices suitable for space and other harsh environments, however the particular gratings fabricated and examined here are not qualified as such. In particular, free-standing, flexible gratings require thicker films than those chosen for these preliminary studies, which are intentionally thin to allow application of the thin-grating equations to the diffraction analysis. The analysis of free-standing gratings on thicker films fabricated by ion irradiation would have to account for variable refractive index with depth in the film. Another common requirement for space-qualified devices is resistance to atomic oxygen, which is unlikely in the devices described here, as thorough oxidation of the irradiated regions is suggested by the SEM images of stained sections in Fig. 4. Development of similar fabrication techniques with alternate polymers would be required to achieve resistance to atomic oxygen and other environmental extremes. Alternative polymers and/or ion beams should also allow for improved optical characteristics. For instance, PMMA film contraction under ion irradiation has been associated with the loss of molecular fragments from the polymer surface.[15] Assuming contraction in the irradiated areas, the achievable phase modulation due to ion irradiation would be maximized with concomitant negative index modulation. The irradiation of PMMA with MeV alpha particles however results in a positive index modulation associated with the formation of unsaturated bonds. Larger index modulation with less shrinkage has been demonstrated due to irradiation of PMMA with heavier ions such as xenon,[15] which however have a much shorter range or penetration depth that would limit the achievable phase modulation. An optimization of these parameters against optical criteria could be performed. It might also be worthwhile to irradiate optical polymers with better rheological properties than PMMA, to determine whether the development of random topographical features in high-dose and/or post-baked gratings is a temperature-induced fluidic process.

The authors would like to thank Xiaoqing Pan, Adriana Lita, and Yu Shen from the University of Michigan Materials Science Department, and Xue-Mei Wang, Hangdong Lee, Joe Kulic, Kent Ross, and Elze Hemmen at TCSUH for technical support.

REFERENCES

1. A. A. Bettiol, T. C. Sum, F. C. Cheong, C. H. Sow, S. V. Rao, J. A. van Kan, E. J. Teo, K. Ansari, and F. Watt, "A progress review of proton beam writing applications in microphotonics," Nucl. Instrum. and Meth. B **231**, 364-371 (2005).
2. A. A. Bettiol, K. Ansari, T. C. Sum, J. A. van Kan, and F. Watt, "Fabrication of micro-optical components in polymer using proton beam writing," in *Micromachining Technology for Micro-Optics and Nano-Optics II*, E. G. Johnson and G. P. Nordin, eds., Proc. SPIE **5347**, 255-263 (2004).
3. A. A. Bettiol, T. C. Sum, J. A. van Kan, and F. Watt, "Fabrication of micro-optical components in polymer using proton beam micro-machining and modification," Nucl. Instrum. and Meth. B **210**, 250-255 (2003).

4. H. Dammann and K. Görtler, "High-efficiency in-line multiple imaging by means of multiple phase holograms," Opt. Commun. **3**(5), 312-315 (1971).
5. L. Zhang, P. D. Townsend, P. J. Chandler, and J. R. Kulisch, "Ion implanted waveguides in polymethylmethacrylate," J. Appl. Phys. **66**(9), 4547-4548 (1989).
6. B. Bennamane, J. L. Decossas, C. Gagnadre, and J. C. Vareille, "Optical waveguide fabrication by ion beams in the PADC-polymer," Nucl. Instrum. and Meth. B **62**, 103-108 (1991).
7. C. Darraud, B. Bennamane, C. Gagnadre, J. L. Decossas, J. C. Vareille, and J. Stejny, "Refractive-index modifications of some polymeric materials by ion beams," Appl. Opt. **33**, 3338-3341 (1994).
8. W. F. X. Frank, F. Linke, A. Schösser, T. K. Strempel, S. Brunner, U. Behringer, T. Tschudi, H. Franke, and T. Sterkenburgh, "Passive optical devices in polymers," Proc. SPIE **2042**, 405-413 (1994).
9. C. V. Raman and N. S. N. Nath, Proc. Indian Acad. Sci. **2**, 406-413 (1935).
10. M. G. Moharam, T. K. Gaylord, and R. Magnusson, "Criteria for Raman-Nath regime diffraction by phase gratings," Opt. Commun. **32**(1), 19-23 (1980).
11. W.-K. Chu, "Energy loss of high-velocity ions in matter," in *Atomic Physics Accelerators*, L. L. Marton and P. Richard, eds., Methods Exp. Phys. **17**, 25-72 (1980).
12. M. Hagiwara and T. Kagiya, "High energy degradation and stabilization of polymers," in *Degradation and Stabilization of Polymers* **1**, 358-388, H. H. G. Jellinek, ed. (Elsevier, 1983).
13. J. H. O'Donnell, "Radiation chemistry of polymers," in *The Effects of Radiation on High-Technology Polymers,* J. H. O'Donnell and E. Reichmanis, eds. (American Chemical Society, 1989), Chap. 1.
14. J. F. Ziegler, J. P. Biersack and U. Littmark, *The Stopping and Range of Ions in Solids*, The Stopping and Ranges of Ions in Matter **1**, J. F. Ziegler, ed. (Pergamon, New York, 1985).
15. R. Kallweit, U. Roll, P. Eichinger, H. Strack, and A. Pöcker, "Correlation between chemical modification and generated refractive index on ion implanted PMMA," in *Materials Modification by Energetic Atoms and Ions,* Mat. Res. Soc. Symp. Proc. **268**, 363-368 (1992).

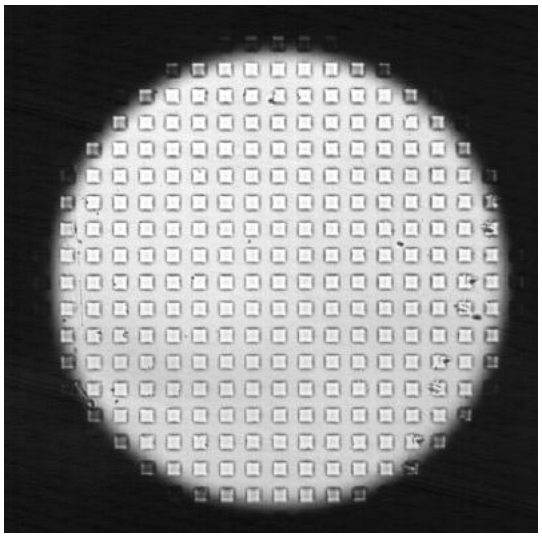

Figure 1. Transmission optical micrograph of a crossed diffraction grating fabricated by patterned ion irradiation of acrylic film. The squares are 7.5µm wide with 5µm separation.

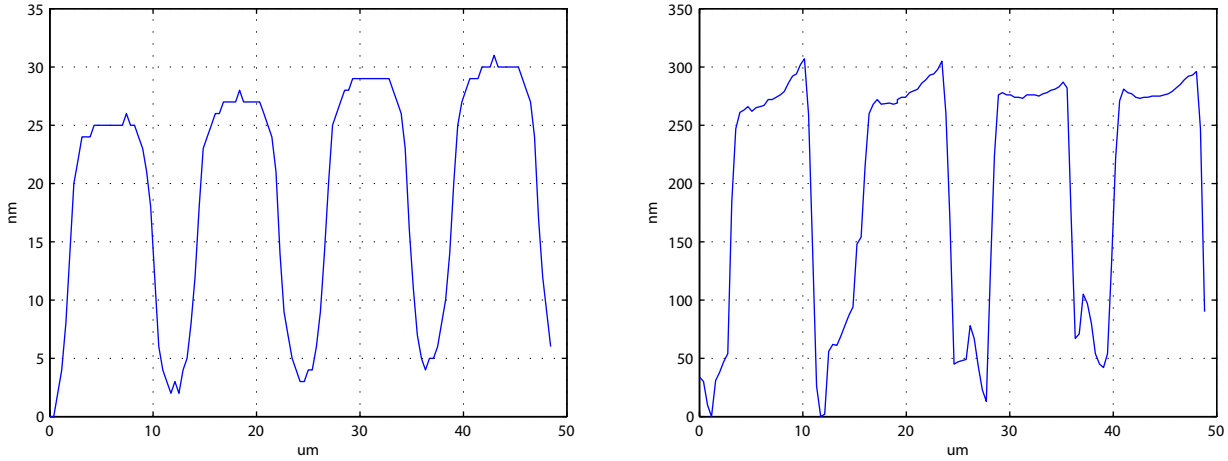

(a) (b)

Figure 2. AFM scans of acrylic gratings produced by irradiation with (a) $3*10^{12}cm^{-2}$ and (b) $7*10^{13}cm^{-2}$ 2MeV alpha particles.

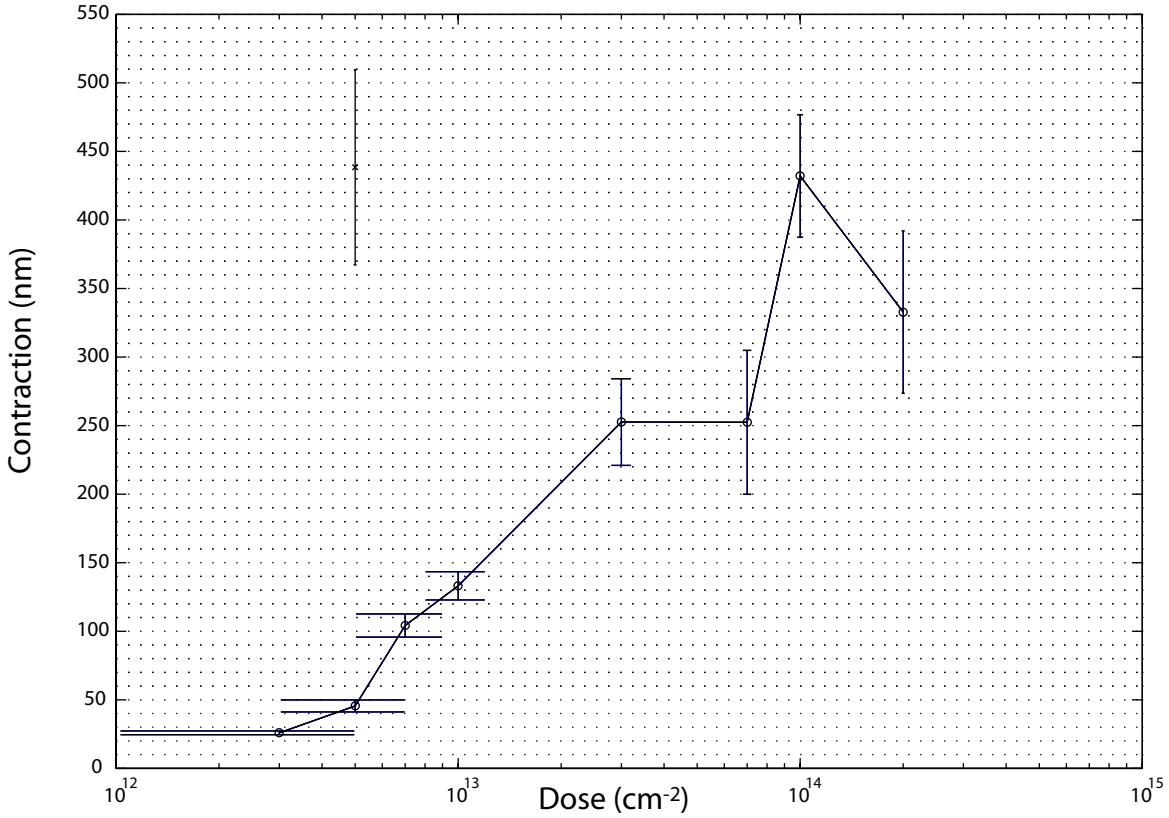

Figure 3. Contraction of PMMA film (3.4μm thick) irradiated to various doses by 2MeV alpha particles in the crossed-grating pattern. Error bars are due to averages over features from 100μm x 100μm AFM scans with 1nm vertical resolution. The data point denoted by 'x' represents the effect of post-irradiation baking.

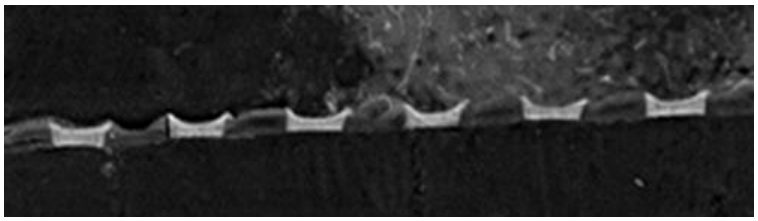

(a)

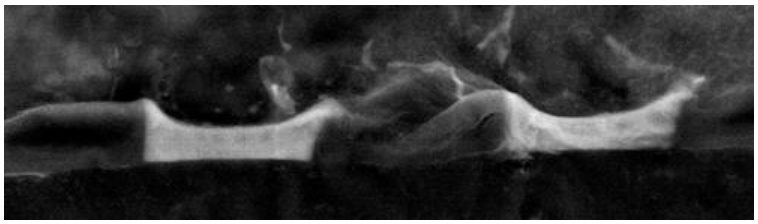

(b)

Figure 4. Scanning electron micrographs, formed by back-scattered electrons, of a stained cross-section of the grating of Fig. 1, which was post-baked. The incident electron energy was 10keV. (a) x 1216 magnification; (b) x 4864 magnification.

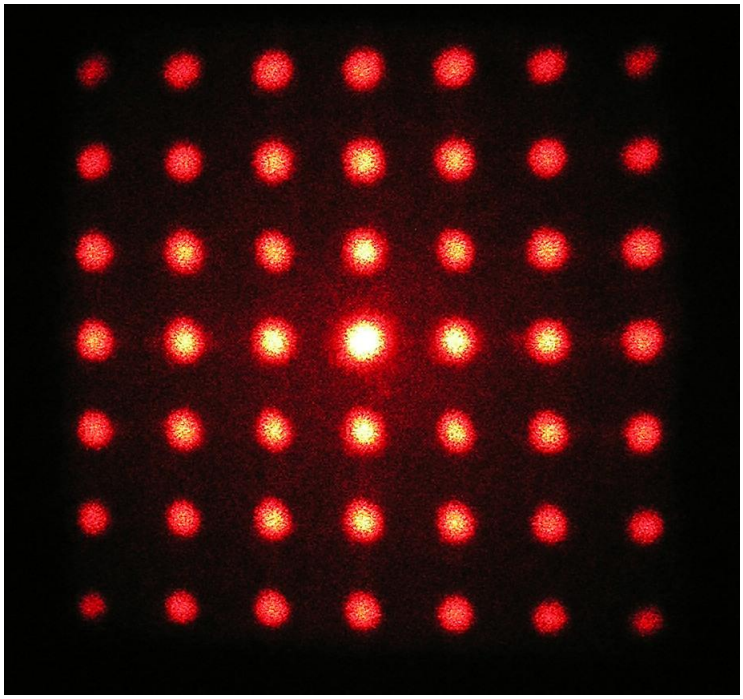

Figure 5. Photograph of a laser spot array generated from a normally-incident helium-neon laser beam by an acrylic grating produced by patterned ion irradiation and post-irradiation baking near the glass transition temperature.

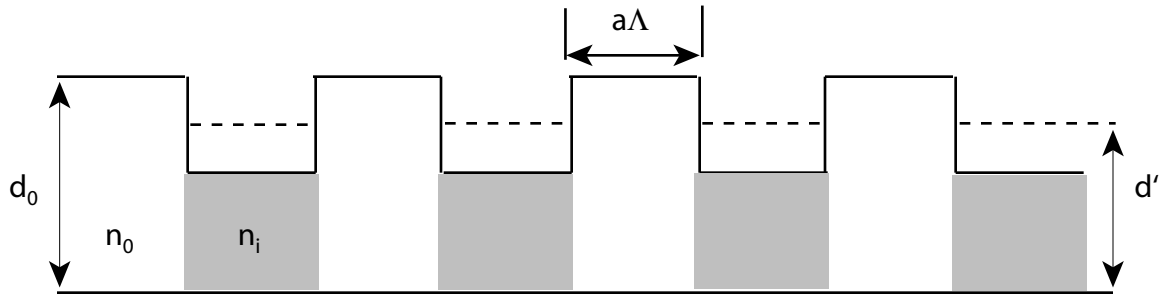

Figure 6. Schematic illustrating parameters used to model the fabricated grating in the thin-grating approximation with a square-wave modulation function.

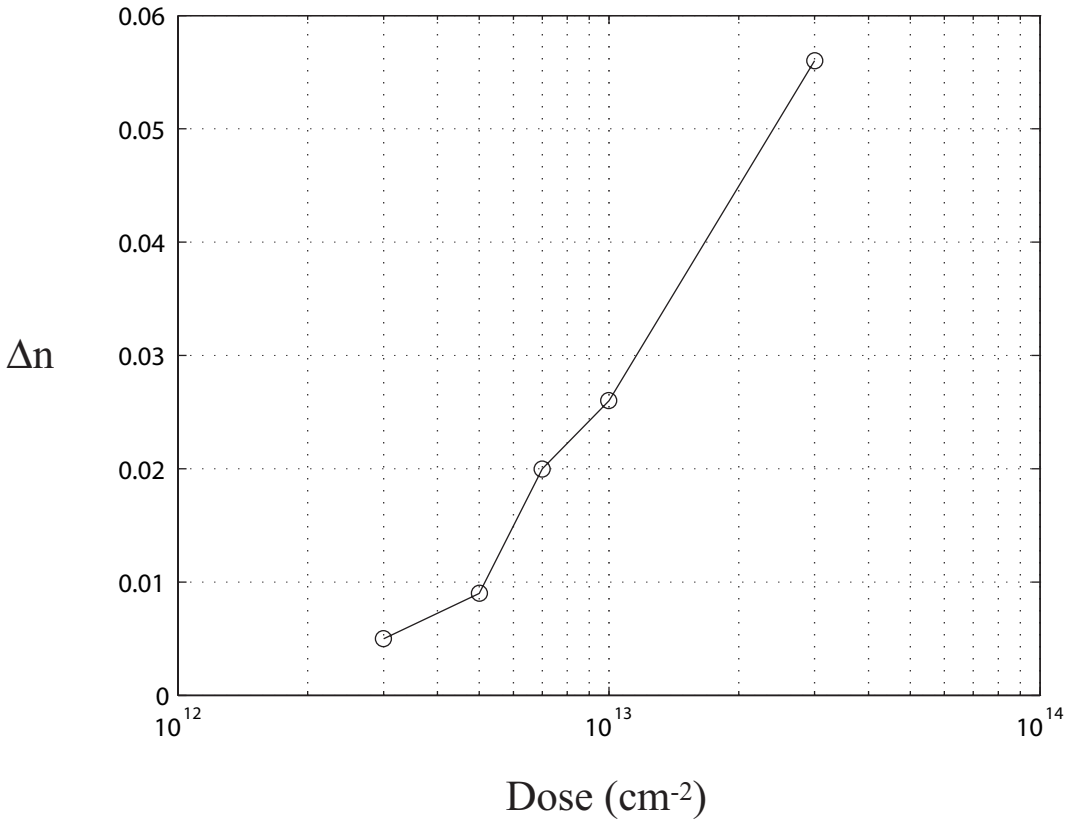

Figure 7. Estimated uniform refractive-index modulation $\Delta n = n_i - n_0$ in 3.4μm-thick PMMA irradiated with 2MeV alpha particles as a function of the dose. $n_0 = 1.490$ is assumed. The errors associated with this data are specified in the text.